Electronic Structure of the Ground and Low-Lying Excited States of TiP

V.-A. Glezakou[†] and Aristides Mavridis*

Laboratory of Physical Chemistry, Department of Chemistry, National and Kapodistrian University of Athens, Post Office Box 64004, 15710 Zographou, Athens, Greece

James F. Harrison*

Department of Chemistry and Center for Fundamental Materials Research, Michigan State University, East Lansing, Michigan 48824-1322

Received: February 21, 1996; In Final Form: May 15, 1996[⊗]

The electronic structure of TiP in its ground $^2\Sigma^+$ and low-lying excited states ($^2\Delta$, $^2\Pi_r$, and $^4\Delta$) has been studied, using MCSCF and multireference CI techniques. We report bond energies, bond lengths, vibrational frequencies, dipole moments, and charge distributions. Additionally, we compare these results with previously reported results for TiN.

Introduction

Interest in the electronic structure of diatomics containing a transition element continues to grow at a significant pace. Information on the bonding in neutral-transition-metal main-group elements is obtained primarily from matrix isolation experiments,[1] gas-phase electronic spectroscopy,[2] and theoretical calculations.[3] We have been active in characterizing the nitrides of the early transition elements,[3a,4] as well as the phosphide and arsenide of Sc,[5] using *ab-initio* electronic structure theory. In this work, we extend these studies to the low-lying electronic states of TiP characterizing the bond energies, bond lengths, charge distribution, dipole moments, and vibrational frequencies. As far as we are aware, there are no experimental data on this molecule.

Preliminaries

Previous studies on TiN[4] suggest that TiP will have a $^2\Sigma^+$ ground state characterized by a triple bond and an unpaired electron on Ti in a σ orbital, and this is what we find. The Lewis structure is

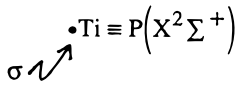

Low-lying excited states may be generated by exciting the nonbonding σ electron to low-lying Ti-based orbitals. Exciting to the $3d_\delta$ will produce a $^2\Delta$, while exciting to the $4p_\pi$ will produce a $^2\Pi$. Note that one cannot excite to a $3d_\pi$ and maintain a triple bond, because these electrons are encumbered in the π bonds. In addition, we have studied the $^4\Delta$, which has the structure

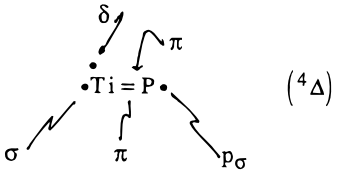

i.e., two π bonds, no σ bond, and three unpaired electrons distributed, as indicated.

TABLE 1: Number of Configuration State Functions Used To Represent Various Electronic States

state	GVB	GVB + 1 + 2	CAS	CAS + 1 + 2
$^2\Sigma^+$ ($^2A_1$)	110	161 491	208	251 086
$^2\Delta$ ($^2A_2$)	76	139 358	196	250 008
$^2\Pi$ ($^2B_1$)	76	143 114	208	250 636
$^4\Delta$ ($^4A_2$)	42	106 542	104	196 353

Computational Details

All calculations were done using the COLUMBUS[6] system of electronic structure codes, as implemented at Michigan State University and The University of Athens. The basis set for Ti is the Wachters[7] 14s, 11p, 5d contracted, following Raffenetti,[8] to 5s, 4p, 2d, and then augmented with a diffuse set of d functions, as recommended by Hay.[9] The final basis is [5s, 4p, 3d]. P is represented by the McLean−Chandler[10] (12, 9, 2) basis, augmented with one even-tempered s and p set, and then contracted to [5, 5, 2] following Raffenetti. In all calculations, we correlated seven electrons, four from Ti and three from P. While the Ti $1s^22s^22p^63s^23p^6$ and the P $1s^22s^22p^63s^2$ "cores" were not correlated, they were, of course, optimized in the GVB (generalized valence bond) and CAS (complete active space) calculations used to generate the orbitals employed in the multireference CI. The CIs were either GVB + 1 + 2 or CAS 7/7 + 1 + 2. The GVB functions we generate differ from the conventional perfect pairing GVB in that we allow all spin couplings. The number of configuration state functions (CSFs) used for each wave function and symmetry are collected in Table 1. An important issue is whether the basis set used is adequate to the task of predicting usefully accurate properties such as frequencies, bond lengths, and dipole moments. A similar basis was used to study TiN,[4a] and these results compared favorably with the results of Bauschlicher,[3a] who used a somewhat larger, one-particle basis.

The total energies calculated for the states of interest are collected in Table 2, while the bond lengths, bond energies, vibrational frequencies, and dipole moments for these states are collected in Table 3. Note that the GVB + 1 + 2 and CAS 7/7 + 1 + 2 results are very similar, and we will focus on the latter. We compare, in Table 4, the CAS + 1 + 2 with recently

[†] Current address: Quantum Chemistry Group, Department of Chemistry, Iowa State University, Ames, IA 50011.

[⊗] Abstract published in *Advance ACS Abstracts,* July 1, 1996.

S0022-3654(96)00526-6 CCC: $12.00

TABLE 2: Total Energies (au) at R_e for Several Electronic States

wave function	$^2\Sigma^+$	$^2\Delta$	$^2\Pi$	$^4\Delta$	separated atoms
GVB	−1189.160 42	−1189.144 30	−1189.109 08	−1189.108 68	−1189.104 56
GVB + 1 + 2	0.23410	0.22629	0.18683	0.18906	0.15973
CAS	0.16175	0.14519	0.11400	0.11065	0.10577
CAS + 1 + 2	0.23433	0.22659	0.18917	0.19035	0.15977

TABLE 3: Bond Lengths, Bond Energies (Relative to Ground-State Products), Dipole Moments, and Vibrational Frequencies for Several Electronic States

	$^2\Sigma^+$				$^2\Delta$				$^2\Pi$				$^4\Delta$			
method	R_e (Å)	D_e (kcal/mol)	μ (D)	ω_e (cm^{-1})	R_e (Å)	D_e (kcal/mol)	μ (D)	ω_e (cm^{-1})	R_e (Å)	D_e (kcal/mol)	μ (D)	ω_e (cm^{-1})	R_e (Å)	D_e (kcal/mol)	μ (D)	ω_e (cm^{-1})
GVB	2.148	35	4.0	430	2.227	25		409	2.447	3		299	2.292	3		368
GVB + 1 + 2	2.149	47	4.5	486	2.218	42	5.3	436	2.299	17	5.9	335	2.237	18	3.2	431
CAS	2.157	35		471	2.223	25		414	2.424	5		291	2.326	3		299
CAS + 1 + 2	2.158	47	4.4	465	2.217	42	7.2	434	2.280	18	5.3	343	2.387	19	3.7	279

TABLE 4: Comparison of Calculated (CI) Spectroscopic Parameters of TiP and TiN

	Lewis	TiN					TiP				
state	structure	R_e (Å)	T_e (eV)	ω_e (cm^{-1})	μ (D)	Q(Ti)	R_e (Å)	T_e (eV)	ω_e (cm^{-1})	μ (D)	Q(Ti)
$^2\Sigma^+$	$\sigma\bullet$Ti≡L	1.613	0.0	1024	3.3	0.50	2.158	0.0	465	4.4	0.48
$^2\Delta$	$\overset{\bullet\delta}{\text{Ti}}\equiv$L	1.657	0.95	931	7.8	0.46	2.217	0.21	434	7.2	0.45
$^2\Pi$	$\overset{4p_\pi\bullet}{\text{Ti}}\equiv$L	1.618	2.01	988	4.4	0.46	2.280	1.23	343	5.3	0.41
$^4\Delta$	$\sigma\bullet\underset{\pi}{\overset{\bullet\delta\pi}{\text{Ti}}}=\text{L}\bullet\sigma$	1.724	1.85	867	2.3	0.49	2.387	1.12	279	3.7	0.44

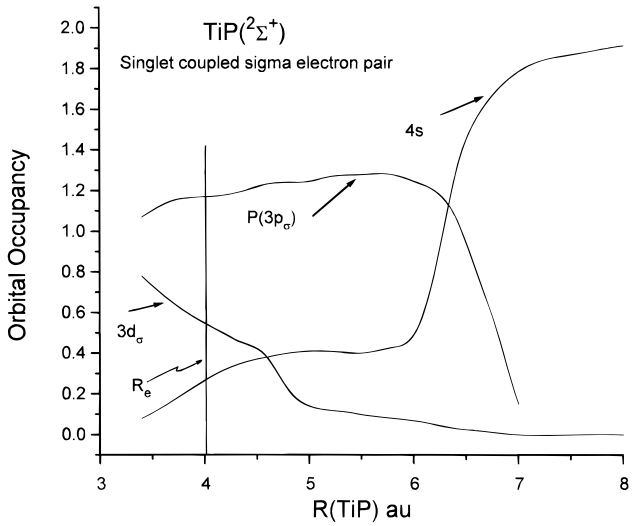

Figure 1. Electron distribution in σ bond of TiP ($^2\Sigma^+$) as a function of internuclear separation, calculated from CAS wave function.

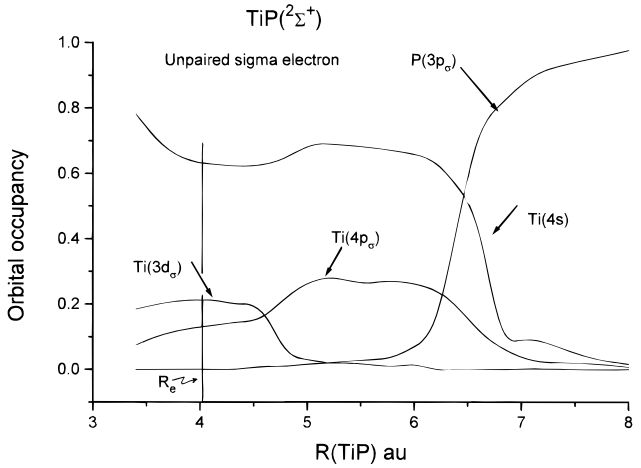

Figure 2. Electron distribution in the unpaired σ orbital of TiP ($^2\Sigma^+$) as a function of internuclear separation, calculated from CAS wave function.

published results for TiN. The geometry has been optimized at each level of theory listed in Table 3.

Discussion

The Ground $^2\Sigma^+$ State. In Figures 1−3, we show the character of the orbital occupation in the σ bond, unpaired σ orbital, and π orbitals, as predicted by the CAS wave function for the $^2\Sigma^+$ state of TiP, as a function of internuclear separation. At large separations, the Ti atom is in the ground ^{3}F ($4s^23d^2$) state, while the P is ^{4}S ($3p^3$), resulting in five high-spin electrons and one singlet coupled pair. At equilibrium, we have three singlet coupled pairs (the triple bond) and one unpaired electron in a σ orbital. As we see in these figures, this transformation from the separated atoms to the molecule is nontrivial. In Figure 1, we track the character of the singlet coupled electron pair in the σ system as it evolves from the Ti $4s^2$ to the TiP σ bond. We have divided this figure into three (somewhat arbitrary) regions: an atomic region (>7 au), a transition region (6−7 au), and a bonding region. Keep in mind that, at large separations, the singlet coupled electron pair is entirely Ti $4s^2$ (except for a near degeneracy contribution involving the 4p orbitals). In Figure 1, the initial encounter in the transition is between the Ti 4s and the P $3p_\sigma$, and we see the 4s electrons going into the P $3p_\sigma$ (charge transfer) and into the Ti $4p_\sigma$ hybridization. As the internuclear separation decreases, we enter the bonding region, where the 4s continues to lose electrons, but now the 4s−4p hybridization begins to decrease as the $3d_\sigma$ occupancy grows.

In Figure 2, we see the evolution of the singly occupied σ electron from the P $3p_\sigma$ at large separation to a metal-localized σ orbital at equilibrium, where it has the composition

$$4s^{0.62}4p_\sigma^{0.14}3d_\sigma^{0.22}$$

Contrast these turbulent transformations in the σ system (Figures 1 and 2) with the gentle evolution of the π system, as represented in Figure 3. Note that the activity in the $3d_\sigma$ orbital

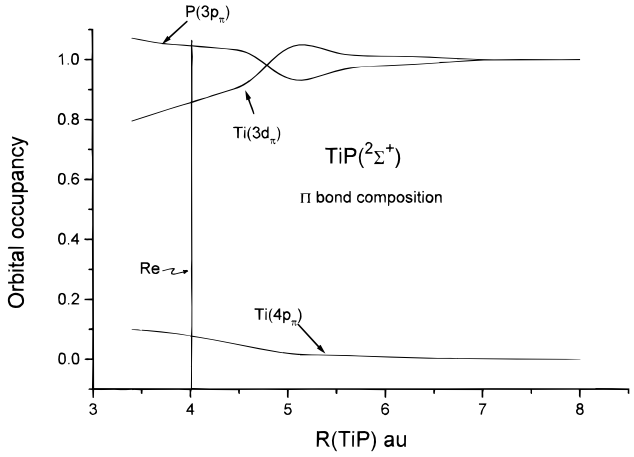

Figure 3. Electron distribution in the bond of TiP ($^2\Sigma^+$) as a function of internuclear separation, calculated from CAS wave function.

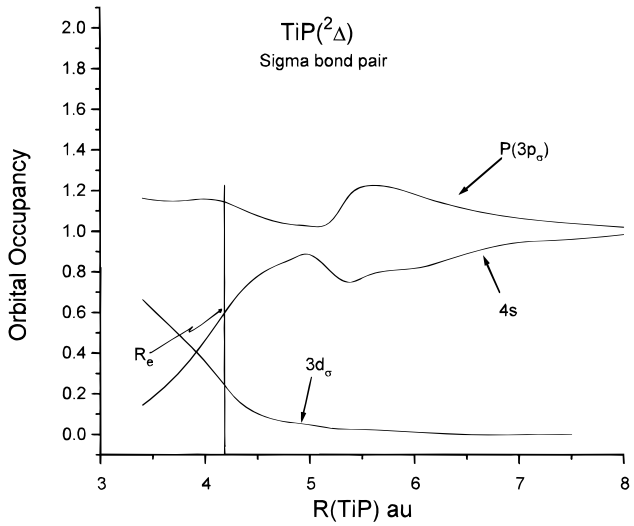

Figure 4. Electron distribution in the σ bond of TiP ($^2\Delta$) as a function of internuclear separation, calculated from CAS wave function.

and the $3d_\pi$ orbitals begins at approximately the same internuclear separations, ~6 au. The net result at equilibrium is that the $^2\Sigma^+$ state is characterized by a triple bond and a singly occupied orbital of σ symmetry, localized on Ti. Ti forms this triple bond using its $3d_\sigma$ and $3d_\pi$ orbitals with the lone σ electron being predominantly 4s with some $3d_\sigma$ and $4p_\sigma$ character. The bonds are polarized toward P, and the Mulliken population suggests that Ti has a charge of +0.48. This is remarkably similar to the Ti charge in TiN (0.50). The σ and π bonds have the approximate orbital occupancies

$$\sigma_{\text{bond}}(^2\Sigma^+) = 4s^{0.28}3d_\sigma^{0.54}3p_\sigma^{1.18}$$

$$\pi_{\text{bond}}(^2\Sigma^+) = 4p_\pi^{0.08}3d_\pi^{0.86}3p_\pi^{1.05}$$

with the $3p_\sigma$ and $3p_\pi$ orbitals on P.

Excited States. Low-lying excited states in which the molecule has a triple bond are easily generated by exciting the electron in the singly occupied σ orbital to primarily metal-based orbitals of π or δ symmetry, forming $^2\Pi$ and $^2\Delta$ states, respectively. In the $^2\Delta$ state, the unpaired electrons is in essentially a pure $3d_\delta$ orbital, and in Figure 4, we track the formation of the σ bond in the $^2\Delta$ state along the diabatic asymptote. Forming a chemical bond in this state is much more direct than in the $X^2\Sigma^+$. At large separation, the singlet coupled σ electrons are the Ti (4s) and P ($3p_\sigma$). As the internuclear separation is decreased, the Ti begins to donate charge, via the σ system, to the P, and this continues unabated until $R \approx 5.5$ au. Up to this point, the σ bond is essentially between 4s and $3p_\sigma$. At 5.5 au, the Ti $3d_\sigma$ begins to participate, and from $R =$ 5.0 to equilibrium, there is a linear decrease in the number of 4s electrons in the bond with a corresponding near linear increase in the number of $3d_\sigma$ electrons. At equilibrium, we have a σ bond that is slightly polarized toward P with the orbital occupation

$$\sigma_{\text{bond}}(^2\Delta) = 4s^{0.60}3d_\sigma^{0.26}3p_\sigma^{1.14}$$

This should be compared to the σ bond composition in the $X^2\Sigma^+$ state,

$$\sigma_{\text{bond}}(^2\Sigma^+) = 4s^{0.28}3d_\sigma^{0.54}3p_\sigma^{1.18}$$

The phosphorus occupation is essentially the same in the two states, while the 4s, $3d_\sigma$ character has reversed in going from $^2\Sigma^+$ to $^2\Delta$.

In Figure 5, we track the formation of the π bond in the $^2\Delta$ state. At 6 au, Ti begins to transfer electrons from its $3d_\pi$ orbital to its $4p_\pi$ orbital, as well as phosphorus' $3p_\pi$ orbital, considerably later than the transfer in the σ system. The net result is that each π bond has the occupancy

$$3d_\pi^{0.77}4p_\pi^{0.09}3p_\pi^{1.14}$$

with P gaining the same number (0.14) electrons from each π orbital as it gained from the σ bond.

The situation with the $^2\Pi$ state is substantially different. Formally, this state is obtained from the $^2\Sigma^+$ by exciting the σ electron to a metal-based $4p_\pi$ orbital. In the resulting $^2\Pi$ state, however, the π electrons readjust so that the unpaired electron is a metal-based $3d_\pi$ and not the $4p_\pi$. The resulting state has the Lewis structure

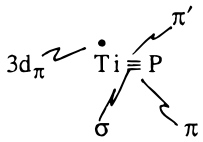

where σ, π, and π' have the approximate orbital occupations

$$\sigma_{\text{bond}}(^2\Pi) = 4s^{0.96}3p_\sigma^{0.94}$$

$$\pi_{\text{bond}}(^2\Pi) = 3d_{xz}^{1.06}3p_x^{0.90}$$

$$\pi'_{\text{bond}}(^2\Pi) = 3d_{yz}^{0.10}4p_y^{0.35}3p_y^{1.54}$$

Asymptotic Products. While all three of these electronic states correlate adiabatically with the ground-state products, Ti (^{3}F) + P (^{4}S), the $^2\Delta$ and $^2\Pi$ states correlate diabatically with excited states of Ti. At equilibium, the $^2\Delta$ state is dominated by the valence electron configuration, $\sigma^2\pi_x^2\pi_y^2\delta^1$ and correlates diabatically with Ti($4s3d^3$), while the $^2\Pi$ has the dominant equilibrium configuration $\sigma^2\pi_y^3\pi_x^2$ and correlates diabatically with Ti ($4s4p3d^2$). The unpaired π_y electron is in a $4p_y$ orbital on Ti.

The last state studied is the $^4\Delta$, with three unpaired electrons, which correlates adiabatically to the ground ^{4}F state of Ti but diabatically to the ^{5}F ($4s3d^3$) and ground-state P. It has no σ bond and two π bonds. All dissociation energies are calculated relative to the adiabatic limits and, therefore, refer to the ground $^4F + {}^4S$ products.

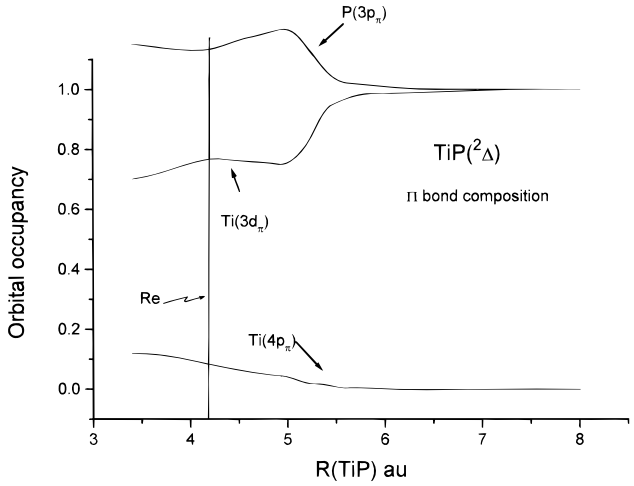

Figure 5. Electron distribution in the π bond of TiP ($^2\Delta$) as a function of internuclear separation, calculated from CAS wave function.

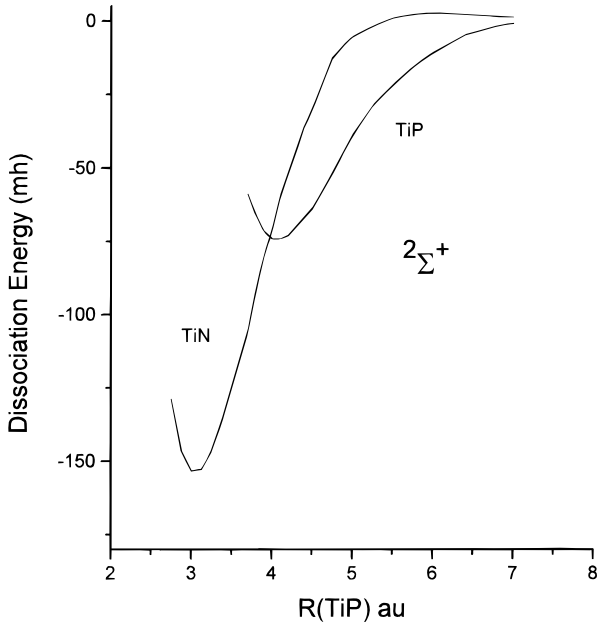

Figure 6. MRCI potential energy curves of TiN and TiP in the $^2\Sigma^+$ state.

Comparison between TiP and TiN Energy Levels. Figure 6 shows the ground $^2\Sigma^+$ potential curves for TiN[4] and TiP. We see that the chemical bond begins to form earlier in TiP than in TiN, primarily because of phosphorus' larger valence p orbital. The larger internuclear separation in TiP is, of course, a consequence of phosphorus' larger "core". At infinite internuclear separation, we can identify the singlet coupled $4s^2$ pair on Ti as the "chemical bond". As the internuclear separation decreases, the character of this singlet coupled pair evolves into a mixture of primarily 4s, 3dσ, and P3pσ orbitals. As we see from Figure 1, the smaller the internuclear separation, the smaller the 4s character in the bond. In TiN, this character goes to zero, while, in TiP, one has 0.28 electrons in the 4s orbital at equilibrium. The electron distribution in the $^2\Sigma^+$ state of TiN and TiP is compared in Table 5.

Figure 7 compares the transition energies (T_e's) calculated for these molecules. As one can see, the relative order of the states is the same, but the T_e's for TiP are substantially smaller than those of TiN. For example, the separation between $^2\Delta$ and $^2\Sigma^+$ in TiN is 0.94 eV, while in TiP it is 0.20 eV. We understand this in a qualitative way, as follows. The ratio of the bond strength of TiP in TiN in the $^2\Sigma^+$ state is calculated to

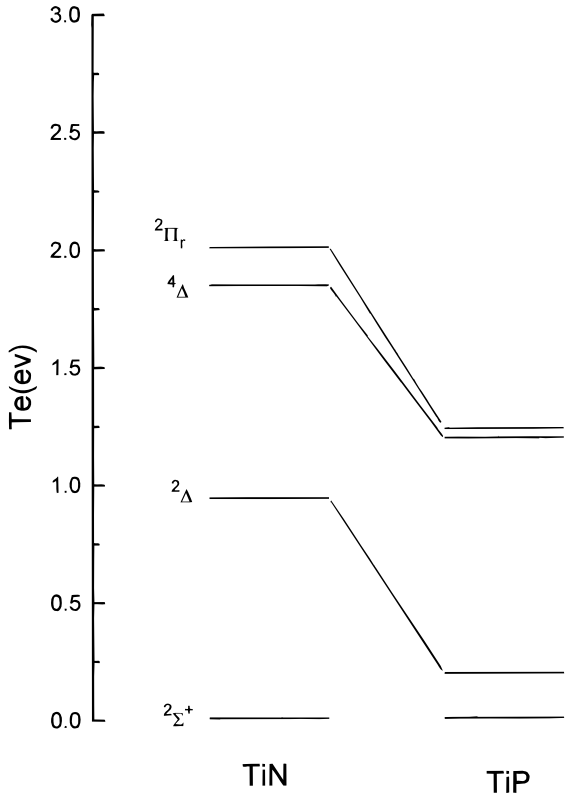

Figure 7. Comparison of the energy separation between the low-lying states of TiN and TiP.

TABLE 5: Comparison of Orbital Populations in the $^2\Sigma^+$ and $^2\Delta$ States of TiN and TiP

		σ bond		π bond		unpaired orbital	
state	orbital	TiN	TiP	TiN	TiP	TiN	TiP
$^2\Sigma^+$	4s	0.00	0.28			0.79	0.62
	4p			0.05	0.08	0.17	0.14
	3d	0.78	0.54	0.75	0.86	0.04	0.22
	ligand p	1.20	1.18	1.20	1.05	0.00	0.00
$^2\Delta$	4s	0.03	0.60				
	4p	0.07	0.00	0.08	0.09		
	3d	0.72	0.26	0.66	0.77	1.0	1.0
	ligand p	1.17	1.14	1.26	1.14		

be 0.48. If this ratio held for the $^2\Delta$ states, we would expect the T_e's to scale by 0.48, which would suggest a T_e of 0.45 eV for the TiP $^2\Sigma^+ - ^2\Delta$ transition. While this model predicts a T_e larger than that explicitly calculated, it does predict the proper trend.

Dipole Moments. The calculated dipole moments, μ, for the four electronic states being cosidered are (in debyes) 4.4 ($^2\Sigma^+$), 7.2 ($^2\Delta$), 5.3 ($^2\Pi$), and 3.7 ($^4\Delta$), all with the polarity Ti^+P^-. This remarkable variation is very similar to that found in TiN[4a] and may be understood in a similar way. When one forms the $^2\Delta$ state from the $^2\Sigma^+$, one moves an electron from the metal-based σ orbital (which is polarized to the rear of Ti away from P) to a metal-based δ orbital whose centroid is essentially at the Ti nucleus. This has the effect of increasing the Ti^+ character in the dipole moment, thus increasing its magnitude. Note the charge on Ti does not vary significantly (+0.50 to +0.48) on going from the $^2\Sigma^+$ to the $^2\Delta$ state, because both the σ and δ orbitals are allocated to Ti in the population analysis. To form the $^4\Delta$ state, one may break the σ bond in the $^2\Sigma^+$ state and place one of these previously bonding electrons in a metal-based δ orbital and the other in a phosphorus $3p_\sigma$ orbital. These two electrons are in orbitals having their centroids on the respective atom and, therefore, do not contribute to the dipole moment. However, since the bonding pair in the $^2\Sigma^+$

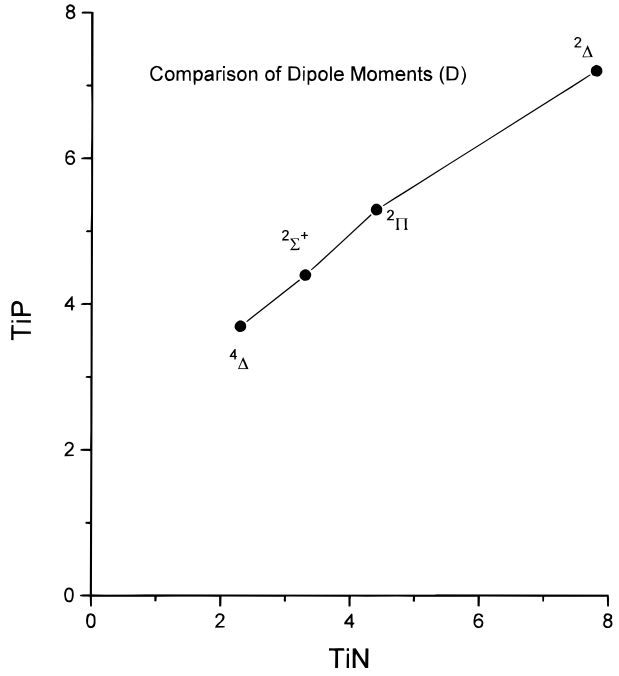

Figure 8. Comparison of calculated dipole moments (from MRCI function) for TiN and TiP.

state was polarized toward P, the net result is to decrease the Ti^+ character in the dipole moment and reduce it below that of the $^2\Sigma^+$ state. The $^2\Pi$ state is obtained from the $^2\Sigma^+$ by exciting the unpaired σ electron into the π system. As noted earlier, the π system in the $^2\Pi$ state is substantially different from the companion $^2\Sigma^+$ and $^2\Delta$ states, in that the unpaired electron is in a metal-based $3d_\pi$ orbital and one of the π bonds involves Ti $4p_\pi$ and P $3p_\pi$ orbitals and is strongly polarized toward P. The dipole moment in the $^2\Pi$ state is larger than that in the $^2\Sigma^+$ state, as expected, but not as large as the dipole in the $^2\Delta$ state, because of the polarization of the Ti $4p_\pi$ orbital in the π bond.

We compare the calculated dipole moments of TiP with those of TiN in Figure 8. The correlation is satisfying.

Conclusion

The electronic structure of TiP is qualitatively similar to that of TiN. Both have a $^2\Sigma^+$ ground state with a first excited state of $^2\Delta$ symmetry. As anticipated, the TiP bond lengths are larger, the vibrational frequencies smaller, and the T_e smaller than the corresponding state of TiN. However, the dipole moments and charge distributions are very similar in TiP and TiN. In particular, while the charge on Ti in each of the four states studied is $\sim+0.5e$, the dipole moments vary from 3.7 to 7.2 D.

Acknowledgment. This work has been supported, in part, by the Michigan State University Center for Fundamental Materials Research and NATO through Award Number 890502. Several of the Silicon Graphics workstations used in this study were purchased with an NSF instrument grant, CHE9321436. J.F.H. acknowledges the partial support of the Michigan State University Special Foreign Travel Fund.

References and Notes

(1) Xiz, Z. L.; Hauge, R. H.; Margrave, J. L. *J. Phys. Chem.* **1992**, *96*, 636. Van Zee, R. J.; Weltner, W., Jr. *J. Am. Chem. Soc.* **1989**, *111*, 4519. Hamrick, Y. M.; Weltner, W., Jr. *J. Chem. Phys.* **1991**, *94*, 3371.

(2) See, for example: Peter, S. L.; Dunn, T. M. *J. Chem. Phys.* **1989**, *90*, 5333. Simard, B.; Masoni, C.; Hackett, P. A. *J. Mol. Spectrosc.* **1989**, *136*, 44. Balfour, W. J.; Merer, A. J.; Niki, H.; Simard, B.; Hackett, P. A. *J. Chem. Phys.* **1993**, *99*, 3288. Ram, R. S.; Bernath, P. F. *J. Chem. Phys.* **1992**, *96*, 6344.

(3) See, for example: (a) Kunze, K. L.; Harrison, J. F. *J. Am. Chem. Soc.* **1990**, *112*, 3812. (b) Bauschlicher, C. W., Jr. *Chem. Phys. Lett.* **1983**, *100*, 515. (c) Mattar, S. M.; Doleman, B. J. *Chem. Phys. Lett.* **1993**, *216*, 369.

(4) (a) Harrison, J. F. *J. Phys. Chem.* **1996**, *100*, 3513. (b) Harrison, J. F.; Kunze, K. L. In *Organometallic Ion Chemistry*; Freiser, B., Ed.; Kluwer Academic Publishers: Dordrecht, 1995.

(5) Tientega, F.; Harrison, J. F. *Chem. Phys. Lett.* **1994**, *223*, 202. Mavridis, A.; Metropoulos, A. *J. Phys. Chem.* **1993**, *97*, 10955.

(6) Shepard, R.; Shavitt, I.; Pitzer, R. M.; Comeau, D. C.; Pepper, M.; Lischka, H.; Szalay, P. G.; Ahlricks, R.; Brown, F. B.; Zhao, J. G. *Int. J. Quantum Chem.* **1988**, *S22*, 149.

(7) Wachters, A. J. H. *J. Chem. Phys.* **1970**, *52*, 1033.

(8) Raffenetti, R. C. *J. Chem. Phys.* **1973**, *58*, 4452.

(9) Hay, P. J. *J. Chem. Phys.* **1977**, *66*, 4377.

(10) McLean, A. D.; Chandler, G. S. *J. Chem. Phys.* **1980**, *72*, 5639.

JP960526Z